EFFECT OF THERMO-MECHANICAL STRESSES ON THE RELIABILITY OF LEAD-FREE LOW SILVER ALLOYS

Morgana Ribas, Ph.D., Anil Kumar, Raghu R. Rangaraju, Divya Kosuri, Pritha Choudhury, Ph.D., Siuli Sarkar, Ph.D.
Alpha Assembly Solutions
Bangalore, KA, India
morgana.ribas@alphaassembly.com

Ranjit Pandher, Ph.D.
Alpha Assembly Solutions
South Plainfield, NJ, USA

Tom Hunsinger
Alpha Assembly Solutions
Somerset, NJ, USA

ABSTRACT
Following regulatory directives that introduced lead-free solder in the electronics manufacturing industry, we built upon the process of developing a lead-free solder alloy that optimizes silver content to improve upon both SAC305 drawbacks and yield cost/pricing. In this work we continue the work of studying the effect of a number of small composition changes to improve Sn-0.3Ag-0.7Cu mechanical properties as well as controlling interfacial intermetallics (IMC) growth and alloy microstructure.

Here we present a comparative analysis between SAC305 and Sn-0.3Ag-0.7Cu-X. We study bulk alloy properties (thermal, mechanical, and others), as well as the effect of drop shock and thermal cycling tests on ball grid array (BGA) and leaded assemblies. The results obtained show that the use of certain additives such as Bi in a low-Ag Sn-Ag-Cu alloy yields an alloy with good mechanical properties, wetting characteristics, good thermal cycling and excellent drop performance. In summary, the additives used in the Sn-0.3Ag-0.7Cu-X alloy were optimized to bridge the gap between Sn-Pb and lead-free alloys thermo-mechanical reliability. Such alloy can be used in a broad set of applications that include semiconductor packaging, consumer electronics, lightening and automotive electronics.

Key words: Lead-free solder, low silver SAC alloy, thermo-mechanical reliability, ball-grid array packages

INTRODUCTION
Hard solders (gold based) were first used in artistic creations sometime between 7,000 and 3,500 BC according to artefacts uncovered from this period. Soft solders (tin-lead) were popularized by the Romans who used it in public works (e.g., aqueducts) and art [1]. From its inception in early 1900's, the electronics industry used Sn-Pb solders in its electronic connections. Eutectic Sn-Pb was a natural choice due to its relatively low cost, good wetting, ability to solder on various types of substrates and just the right melting temperature (183°C) for electronics assembly. Only in the 70's and 80's, health related dangers due to Pb poisoning were uncovered and there was a pressure for its ban. The Safe Drinking Water Act in 1986 introduced the requirement of lead-free plumbing.

It did not take long before the focus shifted to the use of Pb in electronics and the European Union's Restriction of Hazardous Substance (RoHS) directive was introduced in 2001. Two directives were issued by 2006-07: i) Waste of Electrical and Electronic Equipment (WEEE), 2012/19/EU and ii) RoHS, 2002/95/EC. The increasing awareness over environment coupled with availability of reliable lead-free soldering alloys paved the way for many other countries to adopt similar directives as that of EU, as it was the case of USA and Japan.

Upon these regulatory shifts, the electronics manufacturing industry had to adapt and choose the best alternative to eutectic Sn-Pb. Through various consortiums and independent research, SAC305 alloy was established as one of the best cost-benefit lead-free alternatives and became the alloy of choice of the electronics manufacturing industry.

Although SAC305 alloy yields higher thermal cycling reliability than eutectic Sn-Pb it does not match Sn-Pb performance under shock and vibration conditions. To make matters worse, rising and fluctuating price of silver have pressurized the industry to find a low cost (probably with lower silver) solder alloy alternatives. This timeline also coincided with an increasing popularity of portable and hand held electronic devices, which increased emphasis on better reliability of solder joints in drop shock and other high strain rate stresses. SAC305 and other high-silver containing Sn based solders do not have good resistance to

drop shock because of the presence of Sn-Ag intermetallics in the bulk of the solder, which makes such solders relatively brittle. The electronics manufacturing industry quickly realized that there could be an optimum level of silver content to improve upon both SAC305 drawbacks and yield cost/pricing optimization. In process of developing a solder alloy addressing these issues, Alpha focused on using minor alloying additions for improving the mechanical properties of the bulk solder as well as a controlled growth of interfacial IMCs and alloy microstructure.

A Sn-0.3Ag-0.7Cu-Bi alloy was developed in the late 1980's, which was later called SACX 0307. This and other low Ag alloys were proposed as lower cost drop in replacements for SAC305, especially in applications requiring thermal cycling performance of eutectic Sn-Pb or slightly higher. Reducing Ag content resulted in additional mechanical reliability of the solder joints. Further alloying additions on SACX 0307, improved Sn-Ag-Cu alloys mechanical reliability (especially drop performance) even further [2-4].

The shift from eutectic Sn-Pb alloy to lead-free had immediate implications for the electronics industry. Sn-Ag-Cu alloys higher melting point required higher reflow temperatures, from about 220°C to 235-255°C, which resulted in modifications of components and PCB materials [5]. Despite of these challenges, the electronics industry moved forward and quickly adopted Sn-Ag-Cu alloys.

Thus, in addition to obvious economic reasons, such as reduced cost and higher price stability, what would be the implications of using a low-Ag alloy? Here we present a comparative analysis between SAC305 and Sn-0.3Ag-0.7Cu-X. We study bulk alloy properties (thermal, mechanical, and others), as well as the effect of drop shock and thermal cycling tests on ball grid array (BGA) and leaded assemblies.

EXPERIMENTAL DETAILS

The main objective here is to evaluate the suitability of a low-Ag SAC as a drop in replacement for SAC305, and verify the effect of Bi and other additives on thermo-mechanical performance of this alloy. For that, this study is basically divided into four parts: i) Bulk alloy evaluation, ii) Thermal Cycling, iii) Drop Shock, and iv) Solder joint evaluation.

In the bulk alloy evaluation, physical properties (melting point, density, thermal conductivity, electrical resistivity, coefficient of thermal expansion and tensile properties) of Sn-37Pb, SAC305 and Sn-0.3Ag-0.7Cu-X alloy (also named as SACX Plus 0307 SMT) are presented. In the thermal cycling evaluation, upper and lower bounds are defined as SAC305 and Sn-37Pb, respectively. For the drop shock performance evaluation, Sn-37Pb and SAC405 (its higher Ag_3Sn content contributes to lower drop shock compared to SAC305) are upper and lower bounds, respectively. For the solder joint evaluation, Sn-0.3Ag-0.7Cu-X is compared to SAC305, especially on intermetallics thickness and copper dissolution.

Alloy Evaluation

Density was measured by directly measuring volume and mass. The thermal conductivity of the alloys was measured using a Netzsch LFA447 Nanoflash instrument. In this, a xenon flash lamp emits a light pulse that heats the front side of the sample. As the heat generated by absorption of light pulse diffuses through the sample the temperature on the other side of the sample starts increasing. This transient behaviour of temperature is recorded using an infrared detector. The rate of change of temperature depends on the thermal diffusivity (α) of the material, which is then used to calculate the thermal conductivity (K) as $K = \rho.\alpha.c_p$, where ρ is the density and c_p is the specific heat.

Electrical resistivity of the bulk alloys was measured using a four point probe method as per ASTM B193. Samples were machined to 8 mm diameter and a length of 240 mm. The resistance, R, between two points at a distance L apart on the rod was measured and the resistivity was calculated.

The coefficient of thermal expansion (CTE) was measured using a thermal mechanical analyser from TA instruments (model TMA Q400) as per the ASTM E831-06 standard at a ramp rate of 10°C/min. CTE value is taken from the slope of the thermal expansion versus temperature curve from -50°C to +200°C.

Tensile tests were performed at room temperature and 10^{-3} mm/s strain rate as per ASTM E8 standard. An Instron Universal Testing machine (Model 5566) was used to conduct these tests. Samples were preconditioned at 125°C for 48 hrs prior to testing. Three to five specimens of each alloy have been tested and the average values of yield strength, ultimate tensile strength and elongation have been reported.

The ultrasonic pulse-echo technique is used to evaluate the Young's modulus (*E*) of the alloys at room temperature. An ultrasonic thickness gage is used to measure the longitudinal and transverse sound wave velocities through the alloys, which are then used to compute their Young's modulus.

Wetting balance test was conducted in order to assess the effective wetting speed and wetting force as these two parameters can give good insight into solderability performance of the alloy. In the present study SMT coupons were used for the evaluation with standard activated Rosin Flux #2 as per J-STD-003. Prior to testing, all the coupons were preconditioned for 8 hrs, at 72°C/85% temperature humidity followed by 1 hr bake at 105°C in air oven. The wetting results were obtained at 255°C by immersing the test coupons into the solder bath at 45° angle using a Gen3 Must System 3.

Test Vehicle
The test vehicles for thermal cycling and mechanical shock experiments were assembled using the same alloy in ball grid arrays (BGA) and solder paste combination at 240°C peak reflow temperature, and 120s time above liquidus (TAL), using a seven zone reflow oven. Whereas for IMC growth and copper dissolution studies, the test vehicles were consecutively reflowed three times with a peak reflow temperature of 250°C and 120s TAL.

In the present study, the drop shock performance of each alloy was evaluated both on OSP and electrolytic Ni/Au surface finished test vehicles. Each test vehicle used daisy-chained components and board configuration. For studying the effect of accelerated thermal cycling on intermetallics growth and copper dissolution, OSP coated boards with NSMD pads were used, whereas the drop test vehicle had SMD pads. For both investigations, large die (12.06 mm x 12.06 mm) CABGA192 components with 192 I/O's configuration, 0.46 mm ball diameter and 0.8 mm pitch were used. Additional BGA208 components were used for intermetallics growth and copper dissolution evaluation.

Solder joint evaluation of leaded components used an OSP finished PCB. Various components such as SO16, QFP208, PLCC68, and chip resistors 0402 and 1210 were populated under various combinations of TAL (15 to 120s) and peak reflow temperatures (230 to 265°C).

Thermal Cycling
Accelerated thermal cycling test was carried out using an air-to-air thermal shock chamber, from 0°C to 100°C as per IPC 9701A standard, with 10 min ramp and 10 min dwell time for up to 6000 cycles. Electrical failures or discontinuities of the assembled BGA components were continuously monitored using an Agilent multifunction data logger to identify the exact failure point.

Drop Test
Drop test was conducted as per JESD22B111 standard using a drop tester. Each test vehicle had 4 BGA192 components assembled on component locations U2, U4, U12, and U14, which have equivalent fundamental mode of vibration. Each component is tested to failure using 1500G and 0.5 ms shock profile, which is obtained by adjusting the strike surface and drop height. An accelerometer is attached on the drop table near the fixture records the acceleration pulse profile.

The electrical continuity of each component was continuously monitored by using an Analysis Tech event detector. Failures were recorded after at least four subsequent discontinuities, as described in the JEDEC standard. The results are presented through Weibull plots that highlight the failure rates of the alloys.

Solder Joint Evaluation
Failure mode identification was performed on BGA components after thermal cycling and drop shock tests. Representative number of specimens were evaluated by metallographic cross-sectioning preparation and scanning electron microscopy (SEM) analysis.

Assemblies with BGA components were also investigated on the effect of peak reflow temperature and TAL on the intermetallics compound (IMC) growth and base copper dissolution. The quantitative pass criterion was set based on the values derived from the boards that were assembled using high silver sphere-paste combination. The continuous IMC layer thickness was measured for low silver as well as high silver alloys at multiple locations. IMC layer thickness measurements were taken at 12 different locations of the continuous layer and an average is reported (as shown in Figure 1). The target IMC layer thickness is below 7 µm for components reflowed three times with a peak reflow temperature of 250°C and 120s TAL. The base copper dissolution at the board side was evaluated by comparing the copper thickness of unpopulated boards versus the populated boards. Copper dissolution was measured in two regions, under the pad and under the mask, as shown in Figure 1.

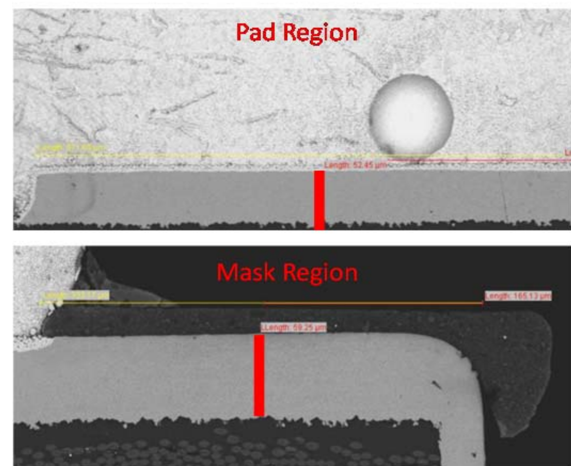

Figure 1. Locations for copper dissolution measurements

Prior to cross-sectioning and microscopic inspection, the leaded components were visually inspected for shorts, opens and other defects. Solder pass criterion was undertaken as per IPC-A-610, section 5.1. Components were evaluated for wetting, maximum fillet height, minimum fillet height, solder thickness and thickness of the lead.

RESULTS AND DISCUSSION
Bulk Alloy Evaluation
Bulk alloy properties of SAC305, Sn-0.3Ag-0.7Cu-X and Sn-37Pb are shown in Table 1. SAC305 melting point is about 38°C higher than of Sn-37Pb, whereas Sn-0.3Ag-0.7Cu-X liquidus temperature is 6.5°C higher than in SAC305. Despite slightly higher liquidus, the solder joint analysis showed that Sn-0.3Ag-0.7Cu-X can be processed under the same reflow conditions of SAC305.

Among their clear advantages, both SAC305 and Sn-0.3Ag-0.7Cu-X have lower CTE, and higher thermal conductivity (K) and lower electrical resistivity (ρ_v) than Sn-37Pb. Yield strength (YS) and ultimate tensile strength (UTS) are also higher than in Sn-37Pb.

Table 1. Bulk alloy properties

Property	SAC305	Sn-0.3Ag-0.7Cu-X	Sn-37Pb
Melting Point, °C	217.3 221.2	217.3 227.6	183 (e)
Density, g/cm^3	7.43	7.33	8.41
K, W/mK	64.0	64.7	50
ρ_v, μΩ.cm	11.80	11.98	14.5
CTE, 10^{-6}/°C	22.8 (-50+200°C)	22.6 (-50+200°C)	24 (30-100°C)
E, GPa	49.9	48.9	15.7#[6]
YS, MPa	34.5	28.9	27.2 [6]
UTS, MPa	39.4	36.5	30.6 [6]
Elongation, %	37.5	37.4	48 [6]

#Obtained from tensile test.

An alloy must exhibit good wetting characteristics on a variety of substrate materials in order to ensure a good solder joint. Here the Sn-0.3Ag-0.7Cu-X alloy wetting is compared to SAC305 as a benchmark. Both alloys presented a zero wetting time below one second, i.e., they pass IPC criterion A as described in the J-STD-003 standard (Figure 2).

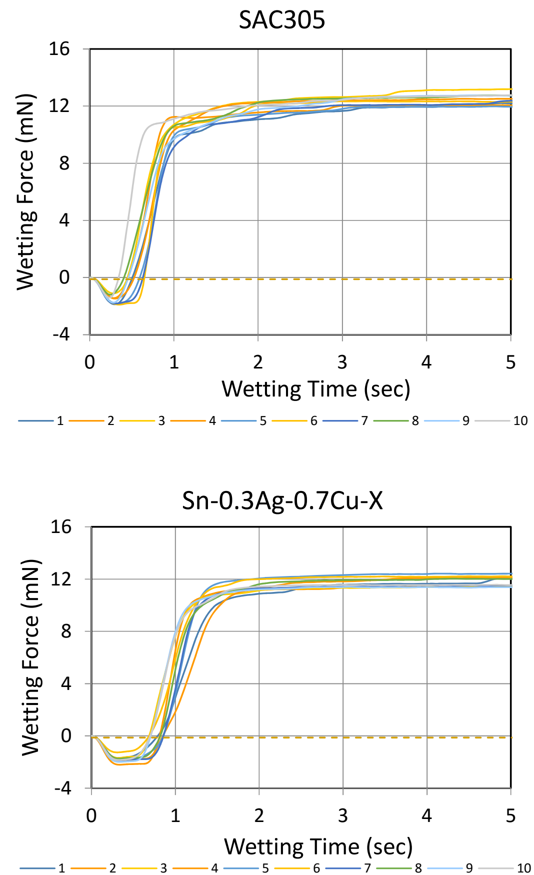

Figure 2. Wetting curves of SAC305 and Sn-0.3Ag-0.7Cu-X

Thermal Cycling

Figure 3 shows the Weibull plot of the Temperature Cycling Test failure data. Sn-37Pb solder joints started failing as early as 665 cycles, whereas SAC305 failed first at 1928 and Sn-0.3Ag-0.7Cu-X at 1866 cycles. All of the Sn-37Pb and Sn-0.3Ag-0.7Cu-X components failed during the 6000 thermal cycles, whereas 23 of SAC305 BGA components survived this test. Sn-0.3Ag-0.7Cu-X thermal cycling characteristic life is 44% higher than Sn-37Pb and 58% lower than SAC305. The observed trend agrees with other independent studies using similar test conditions [7].

Cross-sections analysis of some of the failed components reveals a distinct failure mode for each alloy, as shown in Figure 4. Cracks in SAC305 joints were in the bulk of the solder, near the IMC, either on the PCB or the component side. Sn-0.3Ag-0.7Cu-X and Sn-37Pb also had cracks propagating on the component side. However, cracks in Sn-37Pb joints propagated next to the IMC, on its interface with the bulk, whereas in Sn-0.3Ag-0.7Cu-X joints they were away from the IMC. In case of an actual failure, cracks through the solder joint bulk failures are generally more desirable as their propagation can be controlled by modification of alloy microstructure.

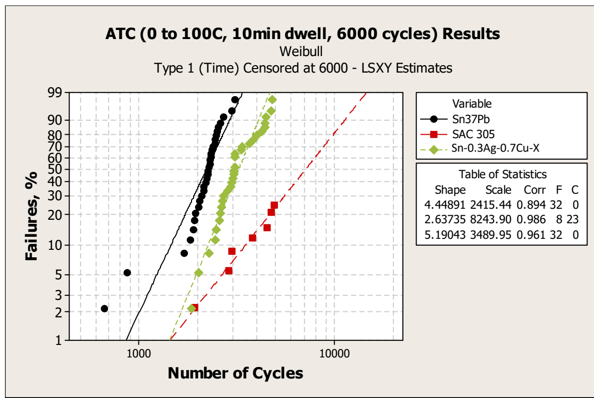

Figure 3. Thermal cycling results

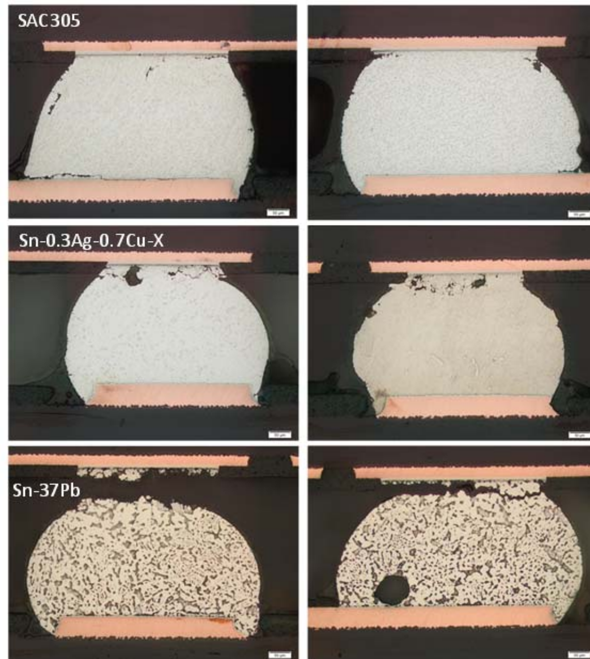

Figure 4. Failure mode after thermal cycling

Drop Shock

A total of 32 BGAs were evaluated for electrical discontinuities as per the JESD22-B111 standard. The results are shown in Weibull plots in Figure 5. On OSP, drop shock performance follows the expected trend, and drop shock characteristic life of Sn-37Pb is 86% higher than SAC405. Sn-0.3Ag-0.7Cu-X alloy characteristic life is 59% higher than SAC405 and only 14% lower than Sn-37Pb.

On electrolytic Ni-Au surface finish, Sn-0.3Ag-0.7Cu-X drop shock characteristic life is 23.5% higher than SAC405 and four times larger than Sn-37Pb. This unusually low resistance to drop shock of Sn-Pb alloy can be understood as a consequence of Au embrittlement. Au embrittlement is well document in Sn-37Pb, leading to degradation of solder joint strength due to brittle Au-Sn intermetallics (most commonly $AuSn_4$ and $AuSn_2$) formation. A generally acceptable level of Au in eutectic Sn-Pb is 3 wt%, below which embrittlement can be avoided [8]. For Sn-Ag-Cu alloys, the limit of Au has been demonstrated to be 5 wt%, below which no embrittlement of solder joint will occur [9].

Through XRF analysis, the corresponding Au content in these PCBs was around 3.3 wt%. Aging of the boards at 125°C for 48h prior to the test has probably accelerated the embrittlement, as shown in reference [10]. Although the Au present in the surface finish was enough to degrade the drop shock performance of Sn-37Pb, its content was not high enough to degrade the low Ag alloy.

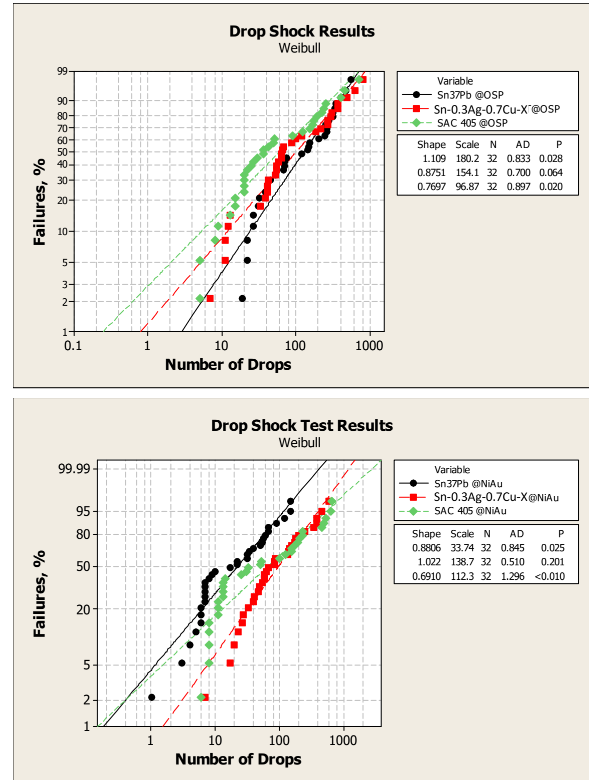

Figure 5. Drop shock performance on OSP (top) and electrolytic Ni-Au (bottom)

Cross-section analysis of some of the failed components revealed the failure modes for each alloy/surface finish combination, as shown in Figures 6 and 7. Similar to other studies evaluating drop shock using SMD pads [11], all components cross-sectioned failed due to clear cracks on the PCB side. Cracks in SAC405 for both OSP and Ni-Au were at the IMC. On OSP, Sn-37Pb showed cracks propagating at the IMC or next to the IMC (i.e., on its interface with the bulk), whereas on Ni-Au the cracks were only at the IMC. For both surface finishes, Sn-0.3Ag-0.7Cu-X had cracks through the solder joint bulk, next to the IMC.

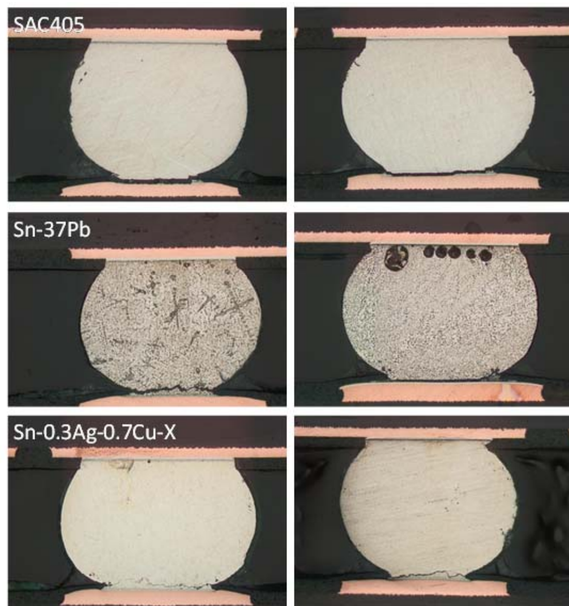

Figure 6. Failure mode after drop shock test @OSP

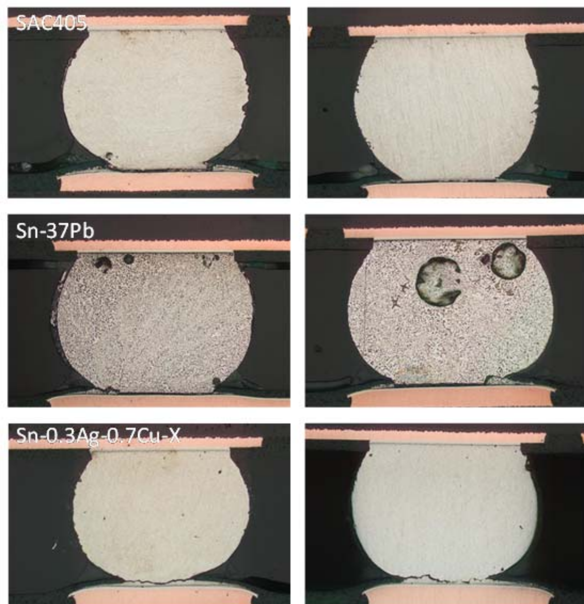

Figure 7. Failure mode after drop shock test @ Ni-Au

Solder Joint Evaluation

Copper thickness results indicating the copper dissolution behaviour of the various alloys are shown in Figure 8. There is a large variation in copper thickness for both populated and unpopulated boards. On the mask region, the variations among the alloys are quite small. However, since these values do not take into account the effect of solder, they are less critical. On the other hand, on the pad area, the effect of solder alloy on copper dissolution is quite clear. Sn-0.3Ag-0.7Cu-X alloy lower Ag content and proprietary additives results in lower copper dissolution than using SAC305. The effect of higher TAL and multiple reflows on intermetallics thickness of Sn-0.3Ag-0.7Cu-X was found to be within acceptable levels. Indeed, due to its lower Ag content and property enhancer additives, even after three times reflow at 250°C and very long TAL (120s), the average intermetallics thickness was below 3 µm (Figure 9).

Further evaluation under wide range of process parameters, TAL (30 to 120s) and temperature (230 to 265°C), demonstrated Sn-0.3Ag-0.7Cu-X fulfils IPC-A-610 requirements. Solder joints voids were below 25% (not quantitatively measured), had good wetting and no solder bridging. For the leaded components, effect of TAL (15 to 120s) and peak reflow temperature (230 to 265°C) was also investigated. Solder joint acceptability was demonstrated by thorough analysis of cross-sections of these components as per IPC-A-610. For all the components, the measured heel fillet height and wetting angle were within the allowable limits. Defects such as solder fillet touching the body of QFP and PLCC were not observed.

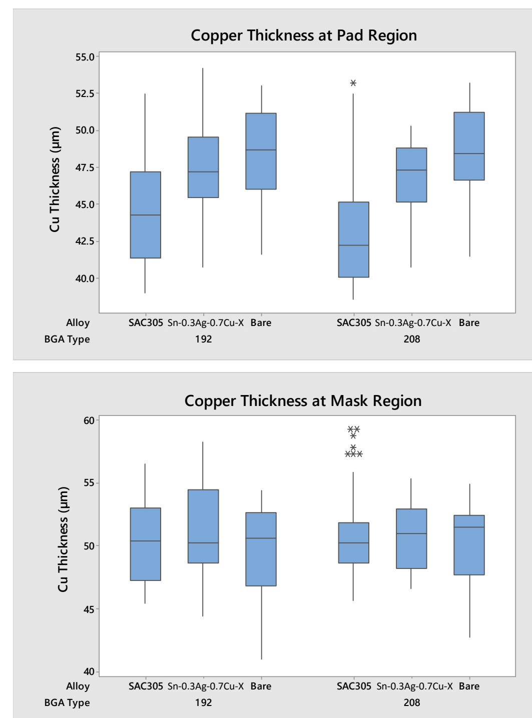

Figure 8. Copper thickness on the pad region (top) and on the mask region (bottom)

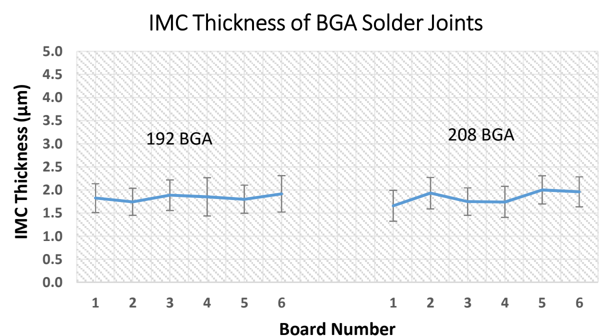

Figure 9. Effect of multiple reflows and longer TAL on intermetallics thickness

CONCLUSIONS

We have presented here a comprehensive evaluation of a Sn-0.3Ag-0.7Cu-X alloy (i.e., SACX Plus 0307 SMT), as both solder paste and spheres. Thermal cycling performance of this alloy is mid-way between Sn-37Pb and SAC305. Moreover, its drop shock performance is 59% higher than SAC405 and just 14% lower than Sn-37Pb on OSP. Other results shown include good wetting, lower copper dissolution than SAC305, and intermetallics thickness after multiple reflow below 3 µm. In summary, it was demonstrated here that the Sn-0.3Ag-0.7Cu-X alloy is very versatile and can be used as a drop-in option in lieu of SAC305, maintaining solder joint performance and thermo-mechanical reliability. Such alloy can be used in a broad set of applications that include semiconductor packaging, consumer electronics, lightening and automotive electronics.

REFERENCES

1. Gilleo K., "The First 7,000 Years of Soldering Part I". Circuits Assembly, October (1994) 30-34.
2. Lall, P. et al., "Interrogation of System State for Damage Assessment in Lead-free Electronics Subjected to Thermo-Mechanical Loads". Proceedings 58th Electronic Components and Technology Conference, Orlando, May, 2008, pp. 918-929.
3. Pandher, R. et al., "Drop Shock Reliability of Lead-Free Alloys - Effect of Micro-Additives". Proceedings 57th Electronic Components and Technology Conference, Reno, May, 2007, pp. 669-676.
4. Pandher, R. and Healey, R., "Reliability of Pb-free Solder Alloys in Demanding BGA and CSP Applications". Proceedings 58th Electronic Components and Technology Conference, Orlando, May, 2008, pp. 2018-2023.
5. Anderson, I. E., "Development of Sn-Ag-Cu and Sn-Ag-Cu-X alloys for Pb-free electronic solder applications". J Mater Sci: Mater Electron, 18 (2007) 55–76.
6. Lead Free Solder Project, National Center for Manufacturing Sciences, 1998.
7. Henshall, G. et al., "Low-Silver BGA Assembly Phase II – Reliability Assessment Sixth Report: Thermal Cycling Results for Unmixed Joints". Proceedings of SMTA International, Orlando, October, 2010.
8. Glazer, J., Kramer, P.A., Morris Jr., J.W., "Effect of Gold on the Reliability of Fine Pitch Surface Mount Solder Joints". Circuit World, 18 (1992) 41 – 46.
9. Pan, J. et al., "Effect of Gold Content on the Reliability of SnAgCu Solder Joints". Proceedings of IPC APEX EXPO, Las Vegas, January, 2011.
10. Mei, Z. et al., "Brittle interfacial fracture of PBGA packages soldered on electroless nickel/immersion gold". Proceedings of 48th Electronic Components & Technology Conference, Seattle, May, 1998.
11. Zhou, T. et al., "Larger Array Fine Pitch Wafer Level Package Drop Test Reliability". Proceedings of InterPACK'09, San Francisco, 2009.

© 2016 MacDermid, Inc. and its group of companies. All rights reserved.
® and ™ are registered trademarks or trademarks of MacDermid, Inc. and its group of companies in the United States and/or other countries.